ORIGINAL PAPER

An analysis of temperature anomalies in Chile using fractional integration

Luis A. Gil-Alana[1,2] · Miguel A. Martin-Valmayor[2,3] · Cristina Hube-Antoine[4]

Abstract

This paper deals with the study of stationarity and mean reversion in the temperature anomalies series in the southwestern American cone. In particular, monthly temperatures in 12 Chilean meteorological stations were studied (from the 1960's to nowadays), examining if temperature shocks are expected to remain in the long term or if they are reversible. The results clearly show a significant relationship between the latitude, climate, and the order of integration of the temperatures. The orders of integration tend to be smaller in colder southern parts, therefore impacts of climate change are expected to be more reversible. However, in northern desert areas the orders of integration are larger than 0.5, thus impacts are expected to be maintained for a longer time.

Keywords Temperature anomalies · Chile · Long memory · Fractional integration

1 Introduction

Chile is a very large country, with three main locations (Continental Chile, the Chilean Islands and Antarctic Chile). In general terms, Continental Chile is a narrowband structure, located between latitudes 17° S and 56° S (more than 4.200 km long), and mainly in the meridional axis of 70° W with a maximum width of only 420 km. It borders physically with the Pacific Ocean marine front in the west and with the very high mountains of the Andes cordillera in the East. This particular structure has led to a wide variation of different climates where precipitation regimes are subject to larger latitudinal variations even on the same parallel, as altitude strongly modulates annual precipitation (Sarricolea et al. 2017). That is why the Chilean climate is of particular interest for the understanding of climate change and its behavior throughout the rest of the world.

Following the IPCC 2014 (Intergovernmental Panel on Climate Change), there seems to be a wide agreement in the International Community about the global warming effect, as from a global perspective, temperatures are tending to increase on Earth. However, in Chile, there is evidence of a particular effect: temperature trends in the southeast Pacific and along the west coast of subtropical South America are tending to cool, but temperatures in continental Chile and Andes cordillera keep rising (Vuille et al. 2015). In particular, the historical temperature trend in central Chile between 1979 and 2005 showed a decrease of − 0.15 °C per decade in the coastal areas, in contrast with the 0.25 °C/decade increase in the mountain range (Garreaud 2011). This particular event and the different types of existing climates in Chile due to its orography leads to a question of particular interest in terms of the impact and duration of temperature shocks in the long term and their relationship with global warming.

We claim first in the paper that the series under analysis display long memory behavior, which is a feature widely observed in climatological time series (Vyushin and Kushner 2009; Zhu et al. 2010; Franzke 2010, 2012; Rea et al. 2011; Yuan et al. 2013; Gil-Alana 2012, 2018, 2022; etc.). In addition, fractional integration is applied to check if the structure of these anomalies is stationary and mean reverting, or even nonstationarity so shocks are expected to

✉ Miguel A. Martin-Valmayor
  mamart02@ucm.es

1 Universidad de Navarra, Pamplona, Spain

2 Universidad Francisco de Vitoria, Madrid, Spain

3 Facultad de Ciencias Económicas y Empresariales, Universidad Complutense de Madrid, 28223 Madrid, Spain

4 Universidad Finis Terrae, Santiago de Chile, Chile

remain in the long term. Moreover, the study of the degree of integration in the series might help to understand how fast this process of convergence is to its original long-term projection, helping climatologists in the construction of models and in the assumptions of future measures.

The paper is structured as follows: Sect. 2 includes a short analysis about the temperatures in Chile. Section 3 is devoted to the methodology. Section 4 describes the dataset, while Sect. 5 displays the main empirical results. Section 6 concludes the manuscript with the main implications of this study.

2 Temperatures in Chile

Existing literature regarding regional temperature analysis is very homogeneous. Salinger (1995) studied the South Pacific by using seasonal and annual changes in temperature using a linear trend, for the 5 decades 1941–1990. He found evidence of a general increase in both daily maximum and minimum temperatures, especially evident in the minimums. He concluded by suggesting that increased concentrations of greenhouse gases and changes in cloudiness could be a plausible mechanism for the overall increase in night-time temperatures. Vuille and Bradley (2000) and Vuille et al. (2003) documented the tendencies of air temperature anomalies from 1939 to 1998 for the tropical Andes, with evidence of a positive linear trend of + 0.11 °C per decade relative to the 1961–1990 mean. More recently, Marengo et al. (2011) analyzed mean annual temperatures and trends in the countries of the northern Andes (Venezuela, Colombia, Ecuador, Peru), with evidence of an increase of about 0.8 °C during the twentieth century. This tendency tends to be greater for climate stations at higher elevations and has tripled over the past 25 years of the twentieth century (+ 0.34 °C per decade), even though some variability appears to be associated with the occurrence of the El Niño Southern Oscillation (ENSO).

Other regional studies have also documented significant warming trends in the Andes over the same period in Peru. Lavado Casimiro et al. (2013) noticed a positive trend in mean temperature of 0.09 °C per decade over the region with similar values in the Andes and rainforest when considering average data, with a significant number of stations with more positive deviations over the Andes region. Salzmann et al. (2013) further examined the Andes analysis with the study of Cordillera Vilcanota glacier (the 2nd largest in Peru), with the overall conclusion of a moderate increase in air temperature, marginal glacier changes between 1962 and 1985, but with a massive ice loss since 1985 (about 45% of volume). Seiler et al. (2013) analyzed the Bolivian region, with homogenized daily

observations of temperature and the impacts of the different climate models in the region (Pacific decadal oscillation (PDO), El Niño-Southern Oscillation (ENSO) and Antarctic Oscillation (AAO)). Temperatures were found to be higher during PDO(+), El Niño and AAO(+) in the Andes, while the number of extreme events were higher during PDO(+), El Niño and La Niña in the lowlands. In general lines, temperatures increased at a rate of 0.1 °C per decade, with stronger increases in the Andes mainly in the dry season. Thibeault et al. (2010) analyzed maximum and minimum temperatures, extreme temperature ranges, frost days, heat wave duration index and warm nights in the Northern Altiplano area (between 16° N and 19° N). Their main results show positive trends in all four indices while trends in warm nights and warm spells are significant, which is consistent with the work in Salinger (1995).

Regarding the specific case of Chile, Rosenbluth et al. (1997) analyzed temperature linear trends computed for the period 1933–1992, with evidence of warming rates from 1.3 to 2.0 °C per 100 years. Moreover, during the last 3 decades warming rates appear to be twice as high as in Salinger (1995) or Thibeault et al. (2010). However, for the specific case of Chile, the generalized warming was not present around 41S, where a cooling period from the 1950s to the 1970s still prevails. Schulz et al. (2012) analyzed Climate Change along the coast of northern Chile over the last century studying the evolution of annual temperature mean anomalies at different pressure levels. Evidence was found of positive trends determined by a strong influence of ENSO, and an abrupt upward shift in the air and ocean temperature regimes in the mid-1970s, coinciding with the change from the cold to the warm phase of the IPO. However, the analysis of a temperature record starting in 1900 revealed no similar changes during other phase changes of the IPO but appears to be similar to that reported for other regions where the temperature regime is also modulated by the IPO (Hartmann and Wendler 2005). Santana et al. (2009) analyzed the specific area of Punta Arenas, with average, maximum and minimum temperatures for the last 120 years. It was found evidence of a slight decrease in the average temperatures, but larger temperature amplitudes and warming/cooling periods from different duration.

More recent studies such as Burger et al. (2018), that focused on the 1979–2010 period, suggest the same evidence of significant warming trends that are widespread at inland stations, while trends are non-significant or negative at coastal sites; Hanna et al. (2017) noticed for the 1979–2006 period a strong contrast between the coastal region (surface cooling: − 0.2 °C per decade) and the Andes region (surface warming: 0.25 °C per decade). Falvey and Garreaud (2009) suggested that this coastal cooling appears to form part of a larger-scale La Niña-like

pattern and there may extend mixed layer below the ocean to 500 m sea depths, generating a temporal cooling at coastal areas in contrast with the general warming pattern across the globe. Meseguer-Ruiz et al. (2019) analysed temperature records in mainland Chile (18 stations from 1966 to 2015) applying Mann–Kendall's non-parametric test. Evidence of positive trends was found for both the minimum and maximum temperature series, especially during the warm months, as in previous studies. However, in the context of global warming, the diverse climatic regions of continental Chile present different behaviors in terms of latitudinal location, lowland/coastal stations and inland/high-elevation stations. Aranda et al. (2021) studied large south central Chilean lakes surface temperatures, with monthly, seasonal, and annual surface temperature trends during the 2000–2016 period, concluding with a significant increase in surface temperature, with a rate of 0.10 °C/decade over the period. Orrego-Verdugo et al. (2021) analyzed temperature amplitudes in the 1985–2015 period with evidence of an increase in maximum temperature from the north (19°S) to the south of Chile (44° S) and in the highlands, in a maximum range of 3.9%, however, the trend is negative in the southern zones (44° S–56° S), with an average value of 12%.

Regarding future expectations and projections, Araya-Osses et al. (2020) looked at climate change projections of temperature and precipitation in Chile based on statistical downscaling, proposing that the entire Chilean territory was under different greenhouse representative concentration pathways. The worst-case scenario (RCP 8.5) implies increments of up to 2 °C and 6 °C for the near future (2016–2035) in the austral winter by the end of the twenty-first century. Mutz et al. (2021) projected similar values (2–7 °C in RCP 8.5), however both studies notify that temperature deviations would be strongly dependent on the RCP scenario (2 °C in RCP 2.6 by the end of the century).

Nevertheless, all the above literature lacks an important feature observed in climatological data including temperatures, this being the long memory issue. This is a property of time series data that implies that observations that are distant in time would be highly dependent. Not taking this feature into consideration may alter the estimation results about linear (or even) nonlinear time trends in the temperatures. Thus, in the present paper, we examined trends in Chilean stations taking also into account this important property of the data, this being the main contribution of the present work.

3 Methodology

In this paper we assume that the series under examination display long memory properties. Long memory, also called long range dependence, is a feature of time series data that is characterized because the observations are highly dependent across time and is a property very often observed in climatological data (see, e.g., Bloomfield 1992; Percival et al. 2001; Caballero et al. 2002; Koutsoyiannis 2003; Langousis and Koutsoyiannis 2006; Gil-Alana 2006, 2012; Franzke 2010; Rea et al. 2011; Bunde and Ludescher 2017; Li et al. 2021; etc.).

Within the long memory class of models, the first applied studies in climatology employed the Hurst exponent (Hurst 1951) or variants of this approach (Koutsoyiannis 2003; Langousis and Koutsoyiannis 2006; López-Lambraño et al. 2018; Chandrasekaran et al. 2019; Benavides-Bravo et al. 2021; etc.). Alternatively, a very popular model is the one based on fractional integration that means that the number of differences to be taken in the series might be any real value thereby including potentially fractional numbers. Thus, a stationary process $\{x_t, t = 0, \pm 1, \ldots\}$ is said to be integrated of order d, and denoted as I(d) if it can be represented as

$$(1 - B)^d x_t = u_t, \quad t = 1, 2, \ldots, \tag{1}$$

where B refers to the backshift operator, i.e., $B^k x_t = x_{t-k}$, and where u_t is integrated of order 0, i.e., I(0) or sometimes called a short memory process. Within the short memory class of models, we can include the white noise and the stationary and invertible AutoRegressive Moving Average (ARMA) class of models. In this latter context, if u_t follows an ARMA(p, q) process, x_t is said to be a fractionally integrated ARMA or ARFIMA(p, d, q) model (Sowell 1992). Recent applications of ARFIMA models in temperature and climatological data include among others the papers by Bhansali and Kolkoszka (2003), Polotzek and Kantz (2020), Asha et al. (2021), etc. Clearly, the main advantage of this methodology is that it is more flexible and general than the classical methods employed in time series analysis which consider only integer degrees of differentiation, i.e., d = 0 in case of stationarity, e.g., ARMA models, and d = 1, in case of nonstationarity, e.g., ARIMA (p, 1, q) models. By allowing d to be any real value, these two cases are incorporated as particular cases of interest, and it permits us to consider more general situations such as stationary long memory processes (if $0 < d < 0.5$) but also nonstationary mean reverting processes (if $0.5 \le d < 1$).

On the other hand, in order to determine if temperatures have increased over time, a classical approach consists of estimating a linear time trend of the form:

$$y_t = \alpha + \beta t + x_t, \quad t = 1, 2, \ldots, \qquad (2)$$

where y_t indicates the observed data (temperature anomalies in our case), and α and β are the coefficients referring respectively to a constant and a linear time trend. In this context, a significant positive value of β indicates support of warming temperatures across time.

Using the above two equations and taking also into account the potential seasonal (monthly) nature of the data, our model specification is one based on the following equation:

$$y_t = \alpha + \beta t + x_t, (1 - B)^d x_t = u_t, u_t = \varphi u_{t-12} + \varepsilon_t, \qquad (3)$$

where y_t is the time series we observe, α and β are unknown coefficients for the intercept and the linear trend; the regression errors x_t are I(d), and u_t is a seasonal (monthly) AR(1) process where φ is the AR coefficient and ε_t is a white noise process.

The differencing parameter d is the measure of the degree of persistence in the data. Thus, the higher its value is, the higher the degree of dependence. Moreover, it permits us to distinguish between mean reversion and lack of it in a more flexible way than the standard methods that only use the values 0 (for stationary series and mean reversion) and 1 (for nonstationarity and lack of it). Mean reversion and no permanent effects of shocks, occurs as long as d is smaller than 1, and the lower the value of d is, the faster the process of convergence is to its original long-term projection. Thus, four different situations can be distinguished:

- if d = 0, the series is short memory, with shocks disappearing relatively fast.
- if 0 < d < 0.5, the series is long memory though still covariance stationary, with shocks last longer than in the previous case.
- if 0.5 ≤ d < 1, the series is no longer covariance stationary though it is still mean reverting with shocks disappearing in the long run
- Finally, if d ≥ 1, the series is not mean reverting and shocks persist forever.

The estimation of d is conducted via the Whittle function in the frequency domain using a parametric approach developed in Robinson (1994). Further details can be seen in Gil-Alana and Robinson (1997) for the functional form of the version of the tests of Robinson (1994) used in this application. Employing alternative methods such as Sowell (1992), Beran (1995) and others produced essentially the same type of results.

4 Data and empirical results

Climatological data were taken from the public site: https://climatologia.meteochile.gob.cl/application/historico/temperaturaHistoricaAnual/330020 where 47 stations were covering the system SACLIM. However, not all these stations have large enough records in temperature data to study persistence and long-term behavior. Thus, only the 10 stations with full temperature records between January 1968 and November 2021 were selected and studied with monthly data, totaling 647 samples. The remaining stations were discarded as they have gaps or their data starts after 2005. As exceptions, Diego Aracena station was also included as its data starts in January 1982 and it was considered good enough with 479 samples, along with Balmaceda which ends at August 2019 and includes 620 samples. The location details of the selected stations are summarized in Table 1.

Sarricolea et al. (2017) analyzed the Continental Chilean climate characteristics following the Köppen–Geiger climate classification, concluding that these climates were essentially arid, temperate, and polar due to the elevation of the Andes, being predominantly high tundra (ET) and mediterranean (Cs). Additionally, with respect to latitude, the climates of northern Chile are mostly arid due to the Atacama Desert, and those of southern Chile tend to be temperate, ranging from Mediterranean to marine west coast. In particular, the locations of the selected stations can be classified in five groups depending on their climate behavior:

I. Norte Grande: between 17° S and 26° S (Arica and Parinacota to Antofagasta) corresponds to a cold desert climate with dry summer, where the temperature frequently exceeds 35 °C. The dryness tends to be limited to the plains; however, a cloudy coastal desert climate is observed towards the coast (from Arica and Parinacota to the Atacama region). Over mountains, a dry-winter tundra climate can be observed over 3000 m above the sea level in the Andes, with a mean annual temperature of 2 °C and cumulative precipitations of 100 mm/year occurring mostly in summer. Over this region, data analyzed was from Chacalluta (Arica—18° S), Diego Aracena (Iquique—20° S), and Cerro Moreno (Antofagasta—23° S), all located in plains.

II. Norte Chico: between 26° S and 32° S (Antofagasta to Coquimbo), there is a cold semi-arid climate with dry summers and oceanic influence towards the coast, where temperatures range from 9 to 20 °C and the mean precipitation is 130 mm/year. Mountains are characterized by a tundra climate with dry

Table 1 Stations included in the study

Name	Code	Height	First data	Last data	Samples
(I) Desert climate (17° S—26 °S)					
1. Chacalluta, Arica Ap	180,005	50.0	Jan-1968	Nov-2021	647
2. Diego Aracena, Iquique	200,006	48.0	Jan-1982	Nov-2021	479
3. Cerro Moreno, Antofagasta	230,001	112.0	Jan-1968	Nov-2021	647
(II) Semi-arid climate (26° S–32° S)					
4. La Florida, La Serena	290,004	137.0	Jan-1968	Nov-2021	647
(III) Mediterranean climate (32° S–40° S)					
5. Quinta Normal, Santiago	330,020	520.0	Jan-1968	Nov-2021	647
6. Pudahuel, Santiago	330,021	482.0	Jan-1968	Nov-2021	647
7. General Freire, Curico	340,031	229.0	Jan-1968	Nov-2021	647
8. Carriel Sur, Concepción	360,019	13.0	Jan-1968	Nov-2021	647
(IV) Marine climate (40° S–44° S)					
9. El Tepual, Puerto Montt	410,005	87.0	Jan-1968	Nov-2021	647
(V) Tundra climate (44° S–56° S)					
10.Teniente Vidal, Coyhaique	450,004	299.0	Jan-1968	Nov-2021	647
11. Balmaceda, Coyhaique	450,005	517.0	Jan-1968	Aug-2019	620
12. Carlos Ibañez, Punta Arenas	520,006	36.0	Jan-1968	Nov-2021	647

summers. La Florida was analyzed over this region (La Serena, 29° S).

III. Zona Central: between 32° S and 40° S (Coquimbo to Araucanía), there is a Mediterranean climate with an annual mean temperature of 15 °C and an annual accumulated precipitation of 150–200 mm. In this region, Quinta Normal, (Santiago, 33° S), Pudahuel (Santiago 33° S), General Freire (Curico, 34° S) and Carriel Sur (Concepción, 36° S) were analyzed.

IV. Zona Sur: between 40° S and 44° S (Araucanía to Los Lagos) the classification corresponds to a marine west coast climate with warm and dry summers, a mean annual temperature of 12 °C and annual precipitation of 2000 mm. Only data for El Tepual, (Puerto Montt 41° S) were available.

V. Sur austral: between 44° S and 56° S (Aysen to Magallanes) experiences a tundra climate, with average temperatures below 0 °C and a mean annual precipitation of 3500 mm. Over this region, the stations at Teniente Vidal (Coyhaique, 45° S), Balmaceda (Coyhaique 45° S) and Carlos Ibañez (Punta Arenas, 52° S) were included.

Figure 1 shows within a map the detail of the locations in terms of the different Chilean climates under study.

Regarding the empirical results, Table 2 displays the estimates of d under the three standard assumptions (in relation to the deterministic terms) of (i) no deterministic terms, i.e., imposing $\alpha = \beta = 0$ in the first equality in (3); (ii) with an intercept ($\beta = 0$) and (iii) with an intercept and a linear time trend. We mark in bold in the table the most adequate specification for each case. In other words, we

estimate the model in Eq. (3) and if α and β both appear statistically significant, we choose that as the selected model. Alternatively, we move to a model with an intercept only, i.e., imposing $\beta = 0$, due to the insignificancy of the time trend coefficient. Table 2 reports the estimated coefficients of the selected model for each series, while Fig. 2 summarizes the average value of d per region, showing evidence of a climatic or latitudinal relationship with d. Significant time trend coefficients are found in the cases of Quinta Normal, Pudahuel, Concepción, Coyhaique, Balmaceda and Punta Arenas. For the remaining cases, the two coefficients of the deterministic terms (constant and time trend) are found to be insignificant. The seasonal effect does not appear as significant in almost any of the series, with a high coefficient being observed at Quinta Normal (0.273).

Looking at Table 3, we see that the highest time trend coefficient corresponds to Pudahuel (0.000285), followed by Quinta Normal (0.00155) and Punta Arenas (0.00151), Balmaceda (0.00122), Concepción (0.00114), and finally Coyhaique (00.00109). Interestingly, all the estimated values of d are found to be higher than 0, implying long memory or long-range dependence.

Moreover, it appears that there is a relationship between latitude and the order of integration as can be seen in Fig. 3, with a very strong R^2 correlation factor between these 12 stations (0.94). The lowest degree of integration and therefore the weakest effect of shocks, correspond to the group of tundra climate (44° S–56° S). In particular, Coyhaique (with an estimated value of d equal to 0.13), Balmaceda (0.14) and El Tepual (0.15). On the other hand, the highest values are those with a desert climate (17° S–
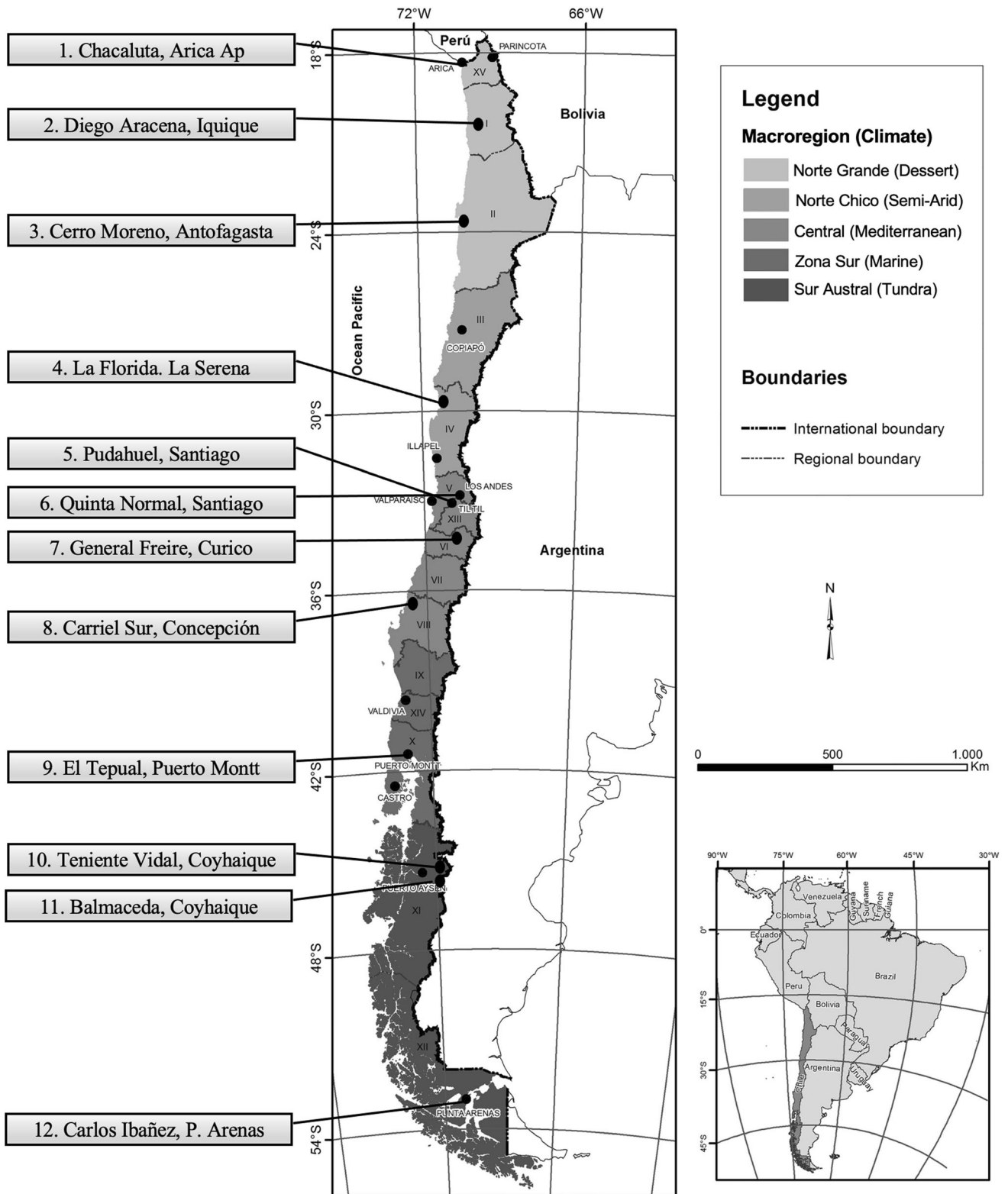
Fig. 1 Detail of the different Chilean climates under study. Taken from Sarricolea et al. (2017) and adapted by authors

26° S) such as Cerro Moreno (0.54), Diego Aracena (0.64) and Chalacuta (0.68). The rest of the regions range between those two limits, but in general lines, with values clearly lower than 0.5.

Table 2 Estimated values of d in the model given by Eq. (1)

Series	No terms	With a constant	With a constant and a linear time trend
(I) Desert climate (17° S–26° S)			
Chalacuta	**0.68 (0.62, 0.76)**	0.68 (0.61, 0.76)	0.68 (0.61, 0.76)
Diego Aracena	**0.64 (0.56, 0.73)**	0.64 (0.56, 0.73)	0.64 (0.56, 0.73)
Cerro Moreno	**0.54 (0.48, 0.61)**	0.54 (0.48, 0.61)	0.54 (0.48, 0.61)
(II) Semi-arid climate (26° S–32° S)			
La Florida	**0.44 (0.38, 0.51)**	0.44 (0.38, 0.51)	0.44 (0.38, 0.51)
(III) Mediterranean climate (32° S–40° S)			
Quinta normal	0.27 (0.22, 0.32)	0.27 (0.22, 0.32)	**0.27 (0.23, 0.30)**
Pudahuel	0.31 (0.27, 0.35)	0.30 (0.27, 0.35)	**0.24 (0.18, 0.30)**
Curico	**0.38 (0.32, 0.46)**	0.38 (0.32, 0.46)	0.38 (0.32, 0.45)
Concepción	0.27 (0.22, 0.33)	0.27 (0.22, 0.33)	**0.25 (0.20, 0.33)**
(IV) Marine climate (40° S–44° S)			
El Tepual	**0.15 (0.09, 0.21)**	0.15 (0.09, 0.21)	0.15 (0.09, 0.21)
(V) Tundra climate (44° S–56° S)			
Teniente Vidal	0.15 (0.10, 0.21)	0.15 (0.10, 0.21)	**0.13 (0.07, 0.19)**
Balmaceda	0.15 (0.10, 0.22)	0.15 (0.10, 0.22)	**0.14 (0.08, 0.21)**
Punta Arenas	0.23 (0.18, 0.28)	0.23 (0.18, 0.28)	**0.19 (0.14, 0.26)**

The values in parenthesis refer to the selected specifications for the deterministic terms

These results appear to be in line with previous studies that notice small positive trends such as Vuille and Bradley (2000) or Vuille et al. (2003, 2015) for the tropical Andes, or the recent work of Orrego-Verdugo et al. (2021) that confirms an increase in the temperatures for northern Chile. In fact, for arid climates our integration factor shows larger values (d > 0.5), implying a possibility of small reversion of this climate change patterns if no external policies are applied. However, as noticed by Schulz et al. (2012) global warming is not present around 41S, where our results might imply stronger mean reverting properties (d < 0.2), suggesting that this cooling pattern might continue in the upcoming future. The physical causes of this pattern are still unclear. Meseguer-Ruiz et al. (2019) points that this issue might be related to the negative Pacific Decadal Oscillation (PDO) phase, the eastern tropical Pacific cooling (Liao et al. 2015), and the modulation induced by the El Niño-Southern Oscillation (ENSO) to the temperatures of the South American Pacific coast (Rosenbluth et al. 1997). Anyway, these empirical results suggest that desert climates appear to be more vulnerable to climate shocks than colder tundra, where these shocks appear to have smaller impacts in the long term. However, the absence of previous studies limits the understanding of the physical mechanisms of these spatial differences and needs further investigation.

Finally, in Table 4 we compare the time trend coefficients obtained throughout the model given by (3) with those obtained imposing the (wrong) assumption that d = 0 in (3).[1] We observe that if long memory is not considered

(i.e., if d = 0), all except one of the series (Cerro Moreno) display significant coefficients, producing erroneous conclusions about the climate in Chile. The temperature increase seems to be overestimated in the desert climate and semi-arid areas while underestimated in the tundra climate areas.

5 Conclusions

The orders of integration of the average monthly temperature deviations time series in eleven Chilean meteorological stations have been calculated, starting in January 1968 until November 2021 with monthly samples, plus an additional one started in January 1982, totaling 647 samples in most cases.

The results obtained, based on fractional integration methods, indicate that there is a significant relationship between the latitude, the climate, and the order of integration of the temperature series. This happens for the specific case of Chile, where generalized global warming was not present around 41S and below, and where a cooling period from the 1950s to the 1970s still prevails (Vuille et al. 2015; Garreaud 2011) specifically in coastal areas. A major limitation of this study has been the absence of long-term data in the Andean stations, where recent studies show a different temperature behavior in comparison with other stations of the same latitude but nearer to

---

[1] Note that the hypothesis of d = 0 has been decisively rejected in the results reported across Tables 3 and 4.
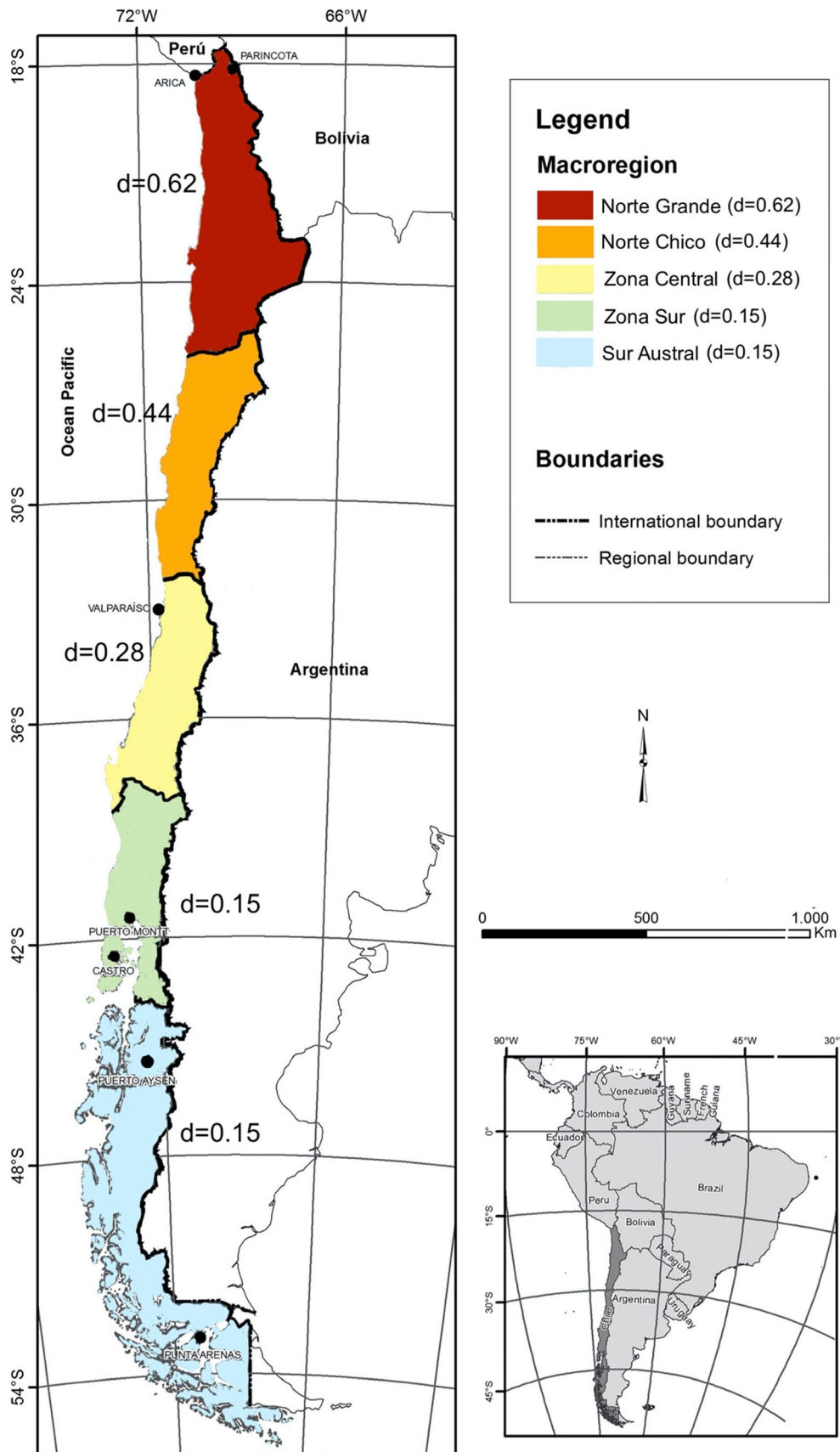
◀**Fig. 2** Average d values obtained per region. Map taken from Sarricolea et al. (2017) and modified by authors

the Pacific coast (Meseguer-Ruiz et al. 2019; Aranda et al. 2021; Orrego-Verdugo et al. 2021, among others). The absence of previous works with this methodology in this

Table 3 Estimated coefficients on the selected model for each series

Series	d (95% band)	Constant (tv)	Time trend tv)	Seas
(I) Desert climate (17° S–26° S)				
Chalacuta	0.68 (0.62, 0.76)	–	–	− 0.057
Diego Aracena	0.64 (0.56, 0.73)	–	–	− 0.071
Cerro Moreno	0.54 (0.48, 0.61)	–	–	− 0.039
(II) Semi-arid climate (26° S–32° S)				
La Florida	0.44 (0.38, 0.51)	–	–	0.082
(III) Mediterranean climate (32° S–40° S)				
Quinta normal	0.27 (0.23, 0.30)	− 0.4876 (− 2.54)	0.00155 (3.14)	− 0.273
Pudahuel	0.24 (0.18, 0.30)	− 0.8497 (− 4.23)	0.00285 (5.53)	− 0.022
Curico	0.38 (0.32, 0.46)	–	–	− 0.053
Concepción	0.25 (0.20, 0.33)	− 0.3058 (− 1.68)	0.00114 (2.24)	0.001
(IV) Marine climate (40° S–44° S)				
El Tepual	0.15 (0.09, 0.21)	–	–	− 0.002
(V) Tundra climate (44° S–56° S)				
Coyhaique	0.13 (0.07, 0.19)	− 0.3627 (− 2.21)	0.00109 (2.57)	− 0.142
Balmaceda	0.14 (0.08, 0.21)	− 0.3862 (− 2.07)	0.00122 (2.43)	0.033
Punta Arenas	0.19 (0.14, 0.26)	− 0.5031 (− 3.09)	0.00151 (3.61)	− 0.097
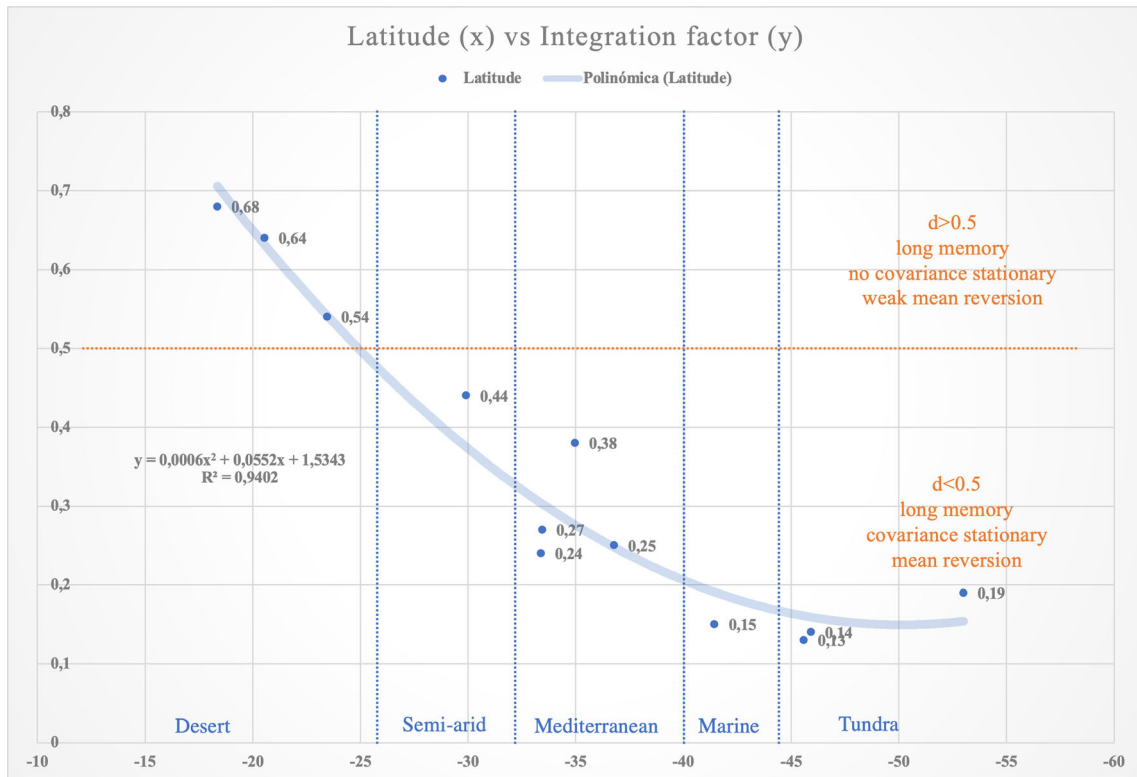
Fig. 3 Empirical relationship between d values obtained and station latitude

Table 4 Time trend coefficient comparisons (d estimated and d = 0)

Series	Time trend with d estimated	Time trend with d = 0
(I) Desert climate (17° S–26° S)		
Chalacuta	–	0.00068 (3.55)
Diego Aracena	–	− 0.00059 (− 2.00)
Cerro Moreno	–	–
(II) Semi-arid climate (26° S–32° S)		
La Florida	–	0.00063 (4.10)
(III) Mediterranean climate (32° S–40° S)		
Quinta normal	0.00155 (3.14)	0.00163 (9.23)
Pudahuel	0.00285 (5.53)	0.00294 (16.50)
Curico	–	− 0.00040 (− 3.02)
Concepción	0.00114 (2.24)	0.00100 (6.37)
(IV) Marine climate (40° S–44° S)		
El Tepual	–	0.00032 (1.85)
(V) Tundra climate (44° S–56° S)		
Coyhaique	0.00109 (2.57)	0.00103 (4.40)
Balmaceda	0.00122 (2.43)	0.00115 (4.34)
Punta Arenas	0.00151 (3.61)	0.00140 (7.90)

part of the globe appears to be a second limitation of this study. However, the results showing low orders of integration specifically in southern latitudes, gives a shadow of hope in the Global Warming policies and in the reversion of these effects, in line with future temperature projections (Araya-Osses et al. 2020; Mutz et al. 2021) that clearly depend on the RCP scenario.

Future works with the same data may analyze the potential presence of non-linearities or structural breaks. These two issues are very much connected with long memory and fractional integration, and the linear trend used in this application can be substituted by alternatives models that might include Chebyshev polynomials in time as in Cuestas and Gil-Alana (2016), Fourier functions in time as in Gil-Alana and Yaya (2021) or even neural networks (Yaya et al. 2021). Work in this direction is now in progress.

and then the calculation and initial discussion of results (tables and point 5). Finally, all authors joined together the conclusions (part 6) and the revision of the manuscript.

Availability of data and materials The authors declare that all data supporting the findings of this study is available within the article and its supplementary information files. In particular, the calculation datasets generated during and/or analyzed during the current study are available from the corresponding author on request. The results/data/figures in this manuscript have not been published elsewhere, nor are they under consideration by another publisher, and there are not hyperlinks to publicly archived datasets analysed or generated during the study except for the public information collected.

Declarations

Ethics approval and consent to participate I declare on behalf of all authors that the manuscript has not been submitted to more than one publication for simultaneous consideration, and that this work is original and has not been published elsewhere in any form or language (partially or in full). Our results are clear, honest, and without fabrication, falsification or inappropriate data manipulation, to discipline-specific rules for acquiring, selecting and processing data. No data, text, or theories by others are presented as if they were the author's own ('plagiarism'). Proper acknowledgements to other works are given (including material that is closely copied), summarized and/ or paraphrased), quotation marks (to indicate words taken from

another source) are used for verbatim copying of material, and permissions secured for material that is copyrighted. I also declare that research articles, relevant literature and non-research articles are cited appropriately. We have avoided untrue statements about entities (who can be an individual person or a company) or descriptions of their behavior or actions that could potentially be seen as personal attacks or allegations about that entity. This research has no threats to public health or national security (e.g. dual use of research). If necessary, we are prepared to send relevant documentation or data in order to verify the validity of the results presented and sensitive information in the form of confidential or proprietary data is excluded. Authors declare all of the above to make sure to respect third parties' rights such as copyright and/or moral rights.

Consent for publication I declare that all authors consent that they are responsible for correctness of the statements provided in the manuscript, as defined by Springer.

Competing interests I declare that the authors have no competing interests as defined by Springer, or other interests that might be perceived to influence the results and/or discussion reported in this paper. In particular, I certify authors have no commercial association, employment or financial involvement that might pose a conflict of interest with regards to the submitted manuscript. All authors certify that they have no affiliations with or involvement in any organization or entity with any financial interest or non-financial interest in the subject matter or materials discussed in this manuscript.

References

Aranda AC, Rivera-Ruiz D, Rodríguez-López L et al (2021) Evidence of climate change based on lake surface temperature trends in south central Chile. Remote Sens 13(22):4535–4535. https://doi.org/10.3390/rs13224535

Araya-Osses D, Uribe JM, M. Paneque M. (2020) Climate change projections of temperature and precipitation in Chile based on statistical downscaling. Clim Dyn 54(9–10):4309–4330. https://doi.org/10.1007/s00382-020-05231-4

Asha J, Kumar SS, Rishidas S (2021) Forecasting performance comparison of daily maximum temperature using ARMA based methods. J Phys Conf Ser 1921. First international conference on advances in smart sensor, signal processing and communication technology (ICASSCT 2021), 19–20, March 2021, Goa, India

Benavides-Bravo FG, Martín-Peon D, Benavides-Rios AG, Walle-Garcia O, Soto-Villalobos R, Aguirre-Lopez MA (2021) A climate-mathematical clustering of rainfall stations in the Río Bravo-San Juan Basin (Mexico) by using the Higuchi fractal dimension and the hurst exponent. Mathematics 9(21):2656

Beran J (1995) Maximum likelihood estimation of the differencing parameter for invertible and short and long memory autoregressive integrated moving average models. J R Stat Soc Ser B 57(4):659–672

Bhansali RJ, Kolkoszka PS (2003) Prediction of long-memory time series. In: Oppenheim G, Taqqu MS, Doukhan P (eds) Theory and applications of long-range dependence. Birkhauser Boston Inc., Boston, pp 355–368

Bloomfield P (1992) Trends in global temperatures. Clim Change 21(1):275–287

Bunde A, Ludescher J (2017) Long-term memory in climate: detection, extreme events, and significance of trends. In: Franzke CLE, O'Kane TJ (eds) Nonlinear and stochastic climate dynamics. Cambridge University Press, Cambridge, pp 318–339

Burger F, Brock B, Montecinos A (2018) Seasonal and elevational contrasts in temperature trends in central Chile between 1979 and 2015. Glob Planet Change 162:136–147. https://doi.org/10.1016/j.gloplacha.2018.01.005

Caballero R, Jewson S, Brix A (2002) Long memory in surface air temperature: detection, modelling, and application to weather derivative valuation. Clim Res 21(2):127–140

Chandrasekaran S, Poomalai S, Saminathan B, Suthanthiravel S, Sundaram K, Hakkim FFA (2019) An investigation on the relationship between the Hurst exponent and the predictability of a rainfall time series. Meteorol Appl 26(3):511–519

Cuestas FJ, Gil-Alana LA (2016) A nonlinear approach with long range dependence based on Chebyshev polynomials in time. Stud Nonlinear Dyn Econom 23:445–468

Falvey M, Garreaud RD (2009) Regional cooling in a warming world: recent temperature trends in the southeast Pacific and along the west coast of subtropical South America (1979–2006). J Geophys Res Atmos 114(4):1–15

Franzke C (2010) Long-range dependence and climate noise characteristics of Antarctic temperature data. J Clim 23(22):6074–6081

Franzke C (2012) Nonlinear trends, long-range dependence, and climate noise properties of surface temperature. J Clim 25(12):4172–4183. https://doi.org/10.1175/JCLI-D-11-00293.1

Garreaud R (2011) Cambio Cimático: Bases físicas e impactos en Chile. Revista Tierra Adentro 93:14

Gil-Alana LA (2006) Nonstationary, long memory and antipersistence in several climatological time series data. Environ Model Assess 11(1):19–29

Gil-Alana LA (2012) Long memory, seasonality and time trends in the average monthly temperatures in Alaska. Theor Appl Climatol 108(3):385–396

Gil-Alana LA (2018) Maximum and minimum temperatures in the United States: time trends and persistence. Atmos Sci Lett 19(4):810–813. https://doi.org/10.1002/asl.810

Gil-Alana LA, Robinson PM (1997) Testing of unit roots and other nonstationary hypothesis in macroeconomic time series. J Econom 80(2):241–268

Gil-Alana LA, Yaya OS (2021) Testing fractional unit roots with nonlinear smooth break approximations using Fourier functions. J Appl Stat 48(13–15):2542–2559

Gil-Alana LA, Gupta R, Sauci L, Carmona-Gonzalez N (2022) Temperature and precipitation in the US states: long memory, persistence, and time trend. Theor Appl Climatol 150:1731–1744

Hanna E, Mernild SH, Yde JC, Villiers S (2017) Surface air temperature fluctuations and lapse rates on Olivares gamma glacier, rio Olivares basin, central Chile, from a novel meteorological sensor network. Adv Meteorol. https://doi.org/10.1155/2017/6581537

Hartmann B, Wendler G (2005) The significance of the 1976 Pacific climate shift in the climatology of Alaska. J Clim 18:4824–4839. https://doi.org/10.1175/JCLI3532.1

Hurst HE (1951) Long-term storage capacity of reservoirs. Trans Am Soc Civ Eng 116:770–799

Koutsoyiannis D (2003) Climate change, the Hurst phenomenon, and hydrological statistics. Hydrol Sci J 48(1):3–24. https://doi.org/10.1623/hysj.48.1.3.43481

Langousis A, Koutsoyiannis D (2006) A stochastic methodology for generation of seasonal time series reproducing overyear scaling behaviour. J Hydrol 322(1–4):138–154. https://doi.org/10.1016/j.jhydrol.2005.02.037

Lavado Casimiro WS, Labat D, Ronchail J, Espinoza JC, Guyot JL (2013) Trends in rainfall and temperature in the Peruvian Amazon-Andes basin over the last 40 years (1965–2007). Hydrol Process 41:2944–2957. https://doi.org/10.1002/hyp.9418

Li X, Sang Y-F, Sivakumar B, Gil-Alana L (2021) Detection of type of trends in surface air temperature in China. J Hydrol 596(2):126061

Liao E, Lu W, Yan XH, Jiang Y, Kidwell A (2015) The coastal ocean response to the global warming acceleration and hiatus. Sci Rep 5:16630. https://doi.org/10.1038/srep16630

López-Lambraño AA, Fuentes C, Lopez-Ramos AA, Mata-Ramirez J, Lopez-Lambraño M (2018) Spatial and temporal Hurst exponent variability of rainfall series based on the climatological distribution in a semiarid region in Mexico. Atmosfera 31(3):199–219

Marengo JA, Pabón JD, Díaz A, Rosas G, Ávalos G, Montealegre E, Villacis M, Solman S, Rojas M (2011) Climate change: evidence and future scenarios for the Andean region. In: Herzog S, Martinez R, Jorgensen P, Tiessen H (eds) Climate change and biodiversity in the tropical Andes. Chapter: 7. IAI – SCOPE

Meseguer-Ruiz O, Corvacho O, Tapia Tosetti A (2019) Analysis of the trends in observed extreme temperatures in mainland Chile between 1966 and 2015 using different indices. Pure Appl Geophys 176:5141–5160. https://doi.org/10.1007/s00024-019-02234-z

Mutz SG, Scherrer S, Ehlers TA (2021) Twenty-first century regional temperature response in chile based on empirical-statistical downscaling. Clim Dyn 56(9–10):2881–2894. https://doi.org/10.1007/s00382-020-05620-9

Orrego-Verdugo R, Abarca-del-Rio R, Lara-Uribe C (2021) Spatial dynamics and consistency of agroclimatic trends in Chile during 1985–2015 to the köppen-geiger climate classification. Chil J Agric Res 81(4):618–629. https://doi.org/10.4067/S0718-58392021000400618

Percival DB, Overland JE, Mofjeld HO (2001) Interpretation of North Pacific variability as a short and long-memory process. J Clim 14(24):4545–4559

Polotzek K, Kantz H (2020) An ARFIMA-based model for daily precipitation amounts with direct access to fluctuations. Stoch Environ Res Risk Assess 34:1487–1505

Rea W, Reale M, Brown J (2011) Long memory in temperature reconstructions. Clim Change 107(3):247–265

Robinson PM (1994) Efficient tests of nonstationary hypotheses. J Am Stat Assoc 89:1420–1437

Rosenbluth B, Fuenzalida H, Aceituno P (1997) Recent temperature variations in southern South America. Int J Climatol 17:67–85

Salinger MJ (1995) Southwest Pacific temperatures: trends in maximum and minimum temperatures. Atmos Res 37(1–3):87–99. https://doi.org/10.1016/0169-8095(94)00071-K

Salzmann N, Huggel C, Rohrer M, Silverio W, Mark BG, Burns P et al (2013) Glacier changes and climate trends derived from multiple sources in the data scarce Cordillera Vilcanota region, southern Peruvian Andes. Cryosphere 7:103–118. https://doi.org/10.5194/tc-7-103-2013

Santana A, Butorovic N, Olave C (2009) Temperature variations in Punta Arenas (Chile) during the last 120 years. Anales Del Instituto De La Patagonia 37(1):85–96. https://doi.org/10.4067/S0718-686X2009000100008

Sarricolea P, Herrera-Ossandón M, Meseguer-Ruiz O (2017) Climatic regionalisation of continental Chile. J Maps 13(2):66–73. https://doi.org/10.1080/17445647.2016.1259592

Schulz N, Boisier JP, Aceituno P (2012) Climate change along the arid coast of northern Chile. Int J Climatol 32(12):1803–1814. https://doi.org/10.1002/joc.2395

Seiler C, Hutjes RWA, Kabat P (2013) Climate variability and trends in Bolivia. J Appl Meteorol Climatol 52(1):130–146. https://doi.org/10.1175/JAMC-D-12-0105.1

Sowell FB (1992) Maximun likelihood estimation of stationary univariate fractionally integrated time series models. J Econom 53:165–188

Thibeault JM, Seth A, Garcia M (2010) Changing climate in the Bolivian Altiplano: CMIP3 projections for temperature and precipitation extremes. J Geophys Res 115:D08103. https://doi.org/10.1029/2009JD012718

Vuille M, Bradley RS (2000) Mean annual temperature trends and their vertical structure in the tropical Andes. Geophys Res Lett 27:3885–3888. https://doi.org/10.1029/2000GL011871

Vuille M, Bradley RS, Werner M, Keimig F (2003) 20th century climate change in the tropical Andes: observations and model results. Clim Change 59(1–2):75–99. https://doi.org/10.1029/2000GL011871

Vuille M, Franquist E, Garreaud R, Casimiro WSL, Cáceres B (2015) Impact of the global warming hiatus on Andean temperature. J Geophys Res Atmos 120(9):3745–3757. https://doi.org/10.1002/2015JD023126

Vyushin DI, Kushner PJ (2009) Power law and long memory characteristics of the atmospheric general circulation. J Clim 22:2890–2904. https://doi.org/10.1175/2008JCLI2528.1

Yaya OS, Ogbonna OE, Furuoka F, Gil-Alana LA (2021) New unit root test for unemployment hysteresis based on the autoregressive neural network. Oxf Bull Econ Stat 83(4):960–981

Yuan N, Fu Z, Liu S (2013) Long-term memory in climate variability: a new look based on fractional integral techniques. J Geophys Res Atmos 118(12):962–969. https://doi.org/10.1002/2013JD020776

Zhu X, Fraedrich K, Liu Z, Blender R (2010) A demonstration of long-term memory and climate predictability. J Clim 23(50):5021–5029. https://doi.org/10.1175/2010JCLI3370.1